Improvement and updating of a cartographic road database by image analysis techniques using multiple knowledge sources and cues

Author(s):
Zhang, Chunsun; Baltsavias, Emmanuel P.

Publication date:
2002

Permanent link:
https://doi.org/10.3929/ethz-a-004333975

Improvement and Updating of a Cartographic Road Database by Image Analysis Techniques using Multiple Knowledge Sources and Cues

Chunsun Zhang and Emmanuel Baltsavias

1 Introduction

The extraction of roads from digital images has drawn considerable attention lately. The existing approaches cover a wide variety of strategies, using different resolution aerial or satellite images. Overviews can be found in GRUEN et al. (1995, 1997) and FOERSTNER & PLUEMER (1997). Semi-automatic schemes require human interaction to provide interactively some information to control the extraction. Roads are then extracted by profile matching (AIRAULT et al. 1996, VOSSELMAN & DE GUNST 1997), cooperative algorithms (MCKEOWN et al. 1988), and dynamic programming or LSB-Snakes (GRUEN & LI 1997). Automatic methods usually extract reliable hypotheses for road segments through edge and line detection and then establish connections between road segments to form road networks (WANG & TRINDER 2000). Contextual information is taken into account to guide the extraction of roads (RUSKONE 1996). Roads can be detected in multi resolution images (BAUMGARTNER & HINZ 2000). The existing approaches show individually that the use of road models and varying strategies for different types of scenes are promising. However, all the methods are based on relatively simplistic road models, and most of them make only insufficient use of a priori information, thus they are very sensitive to disturbances like cars, shadows or occlusions, and do not always provide good quality results. Furthermore, most approaches work in single 2D images, thus neglecting valuable information inherent in 3D processing.

In this paper, we present a knowledge-based system for automatic extraction of 3D roads from two or more aerial images which integrates processing of colour image data and existing digital spatial databases. The information of the existing road database provides a rough model of the scene. Color aerial images give the current situation of the scene, but are complex to analyze without the aid of other auxiliary data. Therefore, the information provided by the existing spatial database can help the understanding of the scene, while the images provide real data useful for improving the old road database and updating it. The system combines different input data that provide complementary, but also redundant information about road existence; therefore, it can account for problematic areas caused by occlusions and shadows, and the success rate and the reliability of the extraction results are increased. The system has been developed within the project ATOMI (**A**utomated reconstruction of **T**opographic **O**bjects from aerial images using vectorized **M**ap **I**nformation), in cooperation with the Swiss Federal Office of Topography (L+T), with aims to improve road centerlines from digitized 1:25,000 topographic maps by fitting them to the real landscape, improving the planimetric accuracy to 1m and providing height information with 1-2m accuracy. The details of ATOMI can be found in EIDENBENZ et al. (2000). We currently use 1:16,000 scale color imagery, with 30cm focal length, and

Paper presented at an AGIT2001 Workshop. In: Fernerkundung und GIS: Neue Sensoren – innovative Methoden, T. Blaschke (Ed.), Wichmann Verlag, Heidelberg, 2001.

60%/20% forward/side overlap, scanned with 14 microns at a Zeiss SCAI. The other input data include: a nationwide DTM with 25m grid spacing and accuracy of 2.5m in the lowlands and 10m in the Alps, the vectorised map data (VEC25) of 1:25,000 scale, and the raster map with its 6 different layers. The VEC25 data have a RMS error of ca. 2.5-7.5m and a maximum one of ca. 12.5m, including generalization effects. They are topologically correct, but due to their partly automated extraction from maps, some errors exist. In addition, DSM data in the working area was generated from stereo images using MATCH-T of Inpho with 2m grid spacing. This paper is organized as following. We describe the general strategy in Section 2, while details for the extraction of various cues are presented in Section 3. Section 4 explains cue combination for road reconstruction and road network generation. In Section 5 results are presented, together with the quality evaluation by comparing the results with manually measured data. The paper is concluded in Section 6 with a discussion and outlook.

2 General Strategy for 3D Road Reconstruction

The developed system makes full use of available information about the scene and contains a set of image analysis tools. The management of different information and the selection of image analysis tools are controlled by a knowledge-based system. The general strategy is shown in Fig. 1.

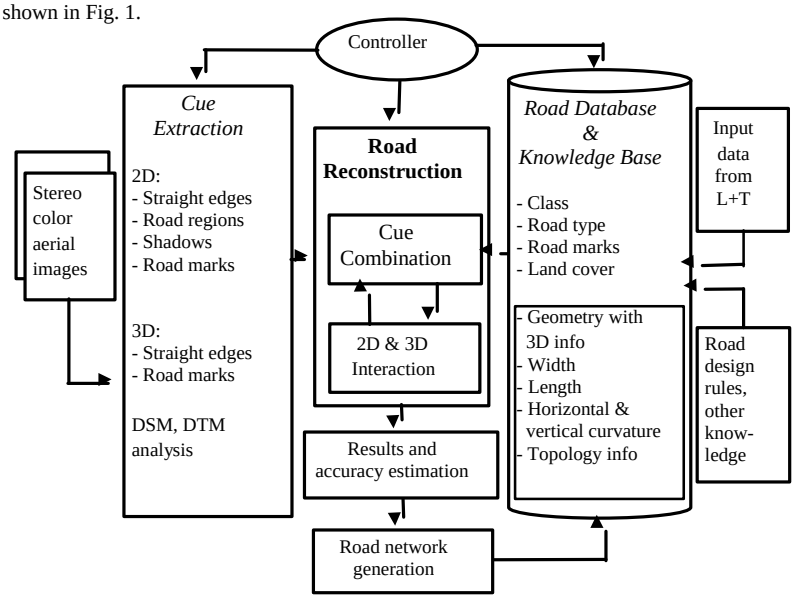

Fig. 1: Strategy of road network extraction in ATOMI.

The initial knowledge base is established by the information extracted from the existing spatial data and road design rules. This information is formed in object-oriented multiple object layers, i.e. roads are divided into various subclasses according to road type, land cover and terrain relief. It provides a global description of road network topology, and the local geometry for a road segment. Therefore, we avoid developing a general road model; instead, a specific model can be assigned to each road segment. This model provides the initial 2D location of a road in the scene, as well as road attributes, such as road class, presence of road marks, land cover and possible geometry (width, length, horizontal and vertical curvature, and so on). A road segment is processed with an appropriate method corresponding to its model, certain features and cues are extracted from images, and roads are derived by a proper combination of cues. The knowledge base is then automatically updated and refined using information gained from previous extraction of roads. The processing proceeds from the easiest subclasses to the most difficult ones. Since neither 2D nor 3D procedures alone are sufficient to solve the problem of road extraction, we make the transition from 2D image space to 3D object space as early as possible, and extract the road network with the mutual interaction between features of these spaces. More details of the general strategy can be found in ZHANG & BALTSAVIAS (2000).

3 Methods for Cue Extraction

When a road segment from VEC25 is selected, the system focuses on the image regions around the road. The regions are defined using the position of the road segment and the maximal error of VEC25. Then, a set of image processing tools is activated to extract features and cues. 3D straight edge generation is a crucial component of our procedure. We are interested in 3D straight edges because the correct road sides are among them. The 3D information of straight edges is determined from the correspondences of edge segments between stereo images. With color images, a multispectral image classification method is implemented to find road regions. We also exploit additional cues such as road marks to support road extraction.

3.1 3D Straight Edge Extraction

Due to the complexity of aerial images, different view angles and occlusions, straight edge matching for 3D edge generation is a difficult task in computer vision and photogrammetry. We developed a structural matching method that exploits rich edge attributes and edge geometrical structure information. The rich edge attributes include the geometrical description of the edge and the photometrical information in the regions right beside the edge (flanking regions). The epipolar constraint is applied to reduce the search space. The similarity measure for an edge pair is computed by comparing the edge attributes. The similarity measure is then used as prior information in structural matching. The locally consistent matching is achieved through structural matching with probability relaxation. We refer to ZHANG & BALTSAVIAS (2000) for the detailed matching strategy.

The input images are first processed with a Wallis filter for contrast enhancement and radiometric equalization (BALTSAVIAS 1991). Edges are extracted using the Canny operator and straight line fitting is applied based on the procedures developed in a previous project (AMOBE, see HENRICSSON (1996)). For each straight edge segment, we

compute the position, length, orientation, and photometric and chromatic robust statistics in the left and right flanking regions. The photometric and chromatic properties are estimated from the “L”, "a" and "b" channels after an RGB to Lab color space conversion and include the median and the scatter matrix.

With known orientation parameters, the epipolar constraint can be employed to reduce the search space. The two end points of an edge segment in one image generate two epipolar lines in the other image. With the approximated height information derived from DTM or DSM data, an epipolar band of limited length is defined. Any edge included in this band (even partially) is a possible candidate, if it intersects the two epipolar lines (through the two edge endpoints in the left image) within this band. The comparison with each candidate edge is then made only in the common overlap length, i.e. ignoring length differences and shifts between edge segments. For each pair of edges that satisfy the epipolar constraints above, their rich attributes are used to compute a similarity score. Therefore, the similarity score is a weighted combination of various criteria. The detailed computation can be found in ZHANG & BALTSAVIAS (2000).

After the computation of similarity measurement, we construct a matching pool and attach a similarity score to each candidate edge pair. Since matching using a local comparison of edge attributes does not always deliver correct results, we developed a structural matching method using probability relaxation. The method seeks the probability that an edge in one image matches an edge in other image, using the geometrical structure information and photometric information of neighbouring image edges. Therefore, the correspondence of both individual edges and edge structures are found. Fig. 2 shows an example of edge extraction and matching. The the extracted straight edges are presented in white, and the matched straight edges are shown in black. More examples and performance evaluation can be found in ZHANG et al. (2001b).

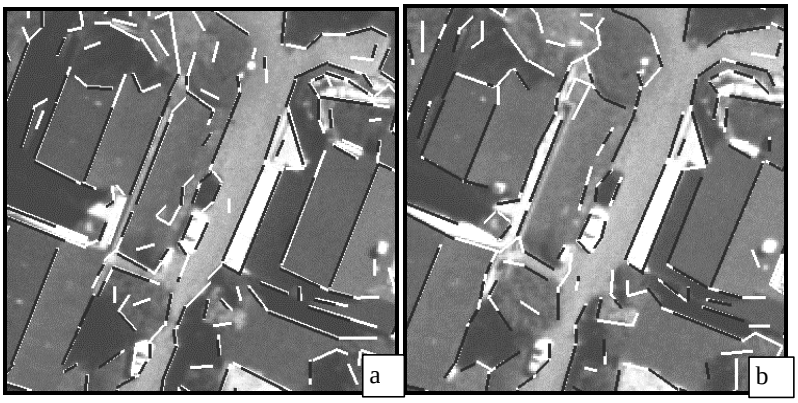

Fig. 2: Straight edge matching: a) left image, b) right image.

The final 3D position of each edge pixel is computed from the original edge pixels and not the fitted straight edges. This is done in the overlap length of the corresponding edges. A 3D straight edge is then fitted to the 3D edge pixels.

3.2 Image Classification for Road Region Detection

We employ the ISODATA (JAIN & DUBES 1988) to classify the images and separate road regions from other objects. The algorithm automatically classifies the image data into desired clusters. It recursively generates a new partition by assigning each pattern to its closest cluster center and merges and splits existing clusters or removes small or outlier clusters. The success of image classification also depends on the data used. As we are concerned with road surfaces and shadows (especially shadows on road surfaces), our purpose is to separate them from other objects in the image, and we do not pay much attention to detect other objects. The original RGB color image is transformed into different color spaces, and the following 3 bands are selected for image classification: 1) a* band from Lab color space, 2) a band calculated with R and G bands in RGB space as (G-R) / (G+R), 3) S band from HSI color space. With this classification, we avoid using a hard threshold for image segmentation, and 5 classes are determined. They correspond to road regions, green objects, shadow areas, dark roofs and red roofs (if available). Fig. 3 is an example of image classification; the roads, shadows, green objects and dark roofs are shown in white, black, dark grey and light grey respectively.

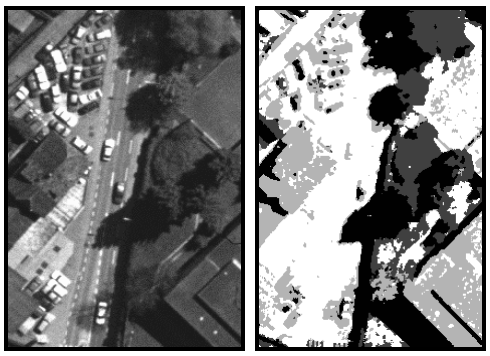

Fig. 3: Example of image classification.

Fig. 4: Subtracting the DTM from DSM.

3.3 DSM and DTM Analysis

We used the DTM or DSM in our system to reduce the search space for straight edge matching. We also use the DSM and DTM to verify if a 3D straight edge is on the ground. Because a DSM ideally models the man-made objects as well as the terrain, subtracting the DTM from DSM results in the seperation of above ground objects (buildings and trees) and

ground objects (roads, etc.). Fig. 4 is an exaple, where above ground objects are shown in bright grey values. By combining this information with image classification data, our system creates redundancy to confirm the existance of roads. Further, it is also used to correct errors in classification data and in occlusion areas the DTM can compensate missing information in the classification data.

3.4 Road Mark and Zebra Crossing Extraction

Road marks and zebra crossings are good indications of the existence of roads. They are generally found on main roads and roads in urban areas. Both of them have distinct color (usually white or yellow). In high resolution images, such as the ones used in our project, road marks are white thin lines with a certain width. The zebra crossings are shown as yellow stripes. As far as road extraction is concerned, road marks give the road direction and often the road centerline, while the zebra crossings define the local road width. Thus, they can be used to guide the road extraction process or verify the extraction results. In addition, in many cases the correct road centerlines can be even derived directly from present road marks and/or zebra crossings. This is especially useful when the roadsides are occluded or not well-defined, such as in cities or city centers. In the following, we describe our developed methods to extract 3D road marks, and the zebra information: the zebra center, the short axis (local road direction), and the long axis (local road width). Note that with the existing knowledge such as DTM, VEC25, and derived information from image processing like DSM and image classification data, the processing can be focused on the road surface within the VEC25 error buffer.

Since road marks are usually white, the image is first segmented by thresholding in R, G, B channels. The road marks are then extracted using an image line model and the geometrical description of each road mark is obtained. The shape of an image line can be presented as a second order polynomial (HARALICK et al. 1983, BUSCH 1994). We can compute the line local direction α using this model. We then obtain the profile in the direction perpendicular to α. The profile can be described as a parabola. Thus, the precise position of each line point is obtained from the profile. The detected line points with similar direction and second directional derivative are linked. The details of the algorithm and implementation can be found in ZHANG et al. (2001a). Straight lines are obtained by least squares fitting. The 3D lines are generated by our developed structural matching method. The 3D lines are then evaluated using knowledge; only those on the ground (as defined by DSM-DTM), belonging to road regions (as determined by the classification) and in the buffer defined by VEC25 are kept as detected road marks.

Zebra crossings are composed of several thin stripes. Again using color information, the image is segmented. Morphological closing is applied to bridge the gaps between zebra stripes. We then obtain several clusters by connected labeling. Only the clusters with a certain size are kept, while the small ones are discarded. The rectangle-like clusters are selected as zebra crossings. The center, short and long axes of the detected zebra crossings are computed using spatial moments.

Fig. 5 is an example of road mark and zebra crossing extraction. The extracted road marks are shown in black lines superimposed on the image. The center, the short and long axes of the detected zebra crossing are also presented.

Fig. 5: Road mark and zebra crossing extraction.

4 Knowledge-based Road Reconstruction: Cue Combination

With the information from existing spatial data and image processing, the knowledge base is established according to the general strategy. The system then extracts roads by finding 3D parallel edges that belong to roadsides and link them in sequence. In case of shadows, occlusions caused by trees and buildings etc., a reasoning process is activated using the knowledge base. Thus, also the cases when only one or no side is visible can be often handled by the system. The main procedures are described below.

The system checks extracted edges to find 3D parallel edges. Only edges located in the buffer defined by VEC25, having a similar orientation to VEC25 segments and a certain slope are further processed. Since roads are on the ground, edges above ground are removed by checking with the DTM. By checking with the image classification results, a relation with the road region (in, outside, at the border) is attached to each edge. Two edges are considered as parallel if they have similar orientation in 3D space. The edges of a pair must overlap in the direction along the edges, and the distance between them must be within a certain range. The minimum and maximum distances depend on the road class defined in VEC25. The found 3D parallel edges are projected onto the images and evaluated using multiple knowledge. The region between the projected edges must belong to the class „road“ as determined by the image classification. If road marks are presented on this road, the extracted road marks are used to confirm that the edge pair corresponds to correct road sides.

For each found 3D parallel edge pair, the system tries to extend them as much as possible using 3D and 2D edge information. And for each extension, a reasoning process (see below) is activated to guarantee that the extension area is road region and extended edges are road sides. The procedures are shown in Fig. 6. We use upper case to represent 3D edge segments, and lower case for 2D edge segments. Suppose that ***ef*** is a 2D straight edge, and ***eg*** is occluded in the other image. Then, we can only generate a 3D straight edge for segment ***gf***, which is shown as ***AB*** in the figure. ***CD*** is another 3D straight edge parallel to ***AB***. Region 1 is the overlap area of ***AB*** and ***CD***, and the system finds that this area belongs to road. Thus, the overlap area is extended to ***C'*** as long as region 2 is also road. Once the system finds with a certain confidence that ***AB*** is a correct road side, region 3 will be checked even if there is no 3D information for segment ***eg***. If region 3 is also road, the overlap area is further extended to ***C"***. The 3D information of point ***e*** is obtained by the

intersection of the image ray passing through ***e***, and the 3D edge ***AB***. This procedure is conducted for 3D segments ***AB*** and ***CD***, and their corresponding 2D straight edges in both images, until there is no possible extension found in 3D and 2D any more. Fig. 7 is an example of extension of parallel edges. The white line are straight edges. The found 3D parallel edge pair is shown in solid black lines. The parallel pair in dotted black lines is generated by extension using a 3D straight edge, while the parallel pair in dotted grey lines (at the lower left part) is generated by extension using a 2D straight edge.

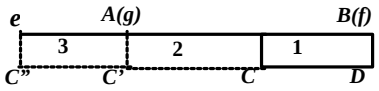

Fig. 6: Extension of parallel edges.

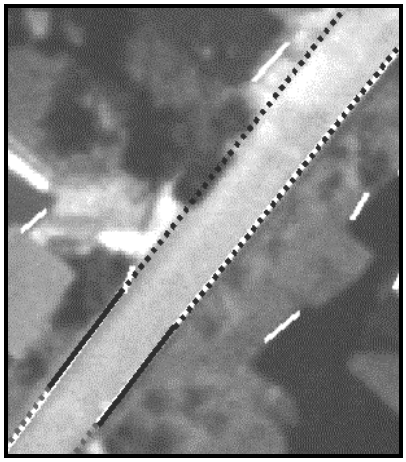

Fig. 7: Example of extension of parallel edges.

The system also checks each individual 3D straight edge, if this edge does not belong to any 3D parallel pair. When one of the sides of the edge is road, the system hypotheses its opposite side using the width from already found 3D parallel edges. Again the hypothesized area is checked using accumulated knowledge. Compared with the visible 3D parallel edges, the system assigns a low reliability to the hypothesized parallel. In case the single visible edge is close to an edge of a found 3D parallel pair and has similar orientation, its reliability is increased.

All found parallel edges are considered as Possible Road Sides that are Parallel (PRSP). They compose a weighted graph. The nodes of the graph are PRSPs, the arcs of the graph are the relations between PRSPs. Note that in occlusion areas, the arcs also represent the missing parts of a road between a pair of PRSPs. The width of two PRSPs should be similar. If there is no gap between two PRSPs, i.e. one PRSP shares points with another, and the linking angles between them in 3D space comply with VEC25, they are connected directly. In case of an existing gap, we first check the connecting angles between PRSPs and the gap. If the angles comply with the VEC25, the gap area is further evaluated using additional information, and we compute the possibility of the gap belonging to road. This is called reasoning process in our work. If the gap is not too long, and

- within the gap is a road region, or
- within the gap is a shadow or shadow mixed with road region, or
- the gap is caused by tree occlusion (determined from the image classification results and DSM-DTM), or
- within the gap is terrain as determined by the DSM-DTM, or
- road marks are extracted within the gap

then, we consider the gap as possibly belonging to a road. Suppose N is the total number of pixels in the gap, and Nr, Ns are numbers of pixels of road and shadow respectively. The possibility of the gap belonging to a road is computed as $P_g = S_g * S_p$, where S_g and S_p are measures using height and image information respectively. They are given as

$$S_g = \frac{\sum\left(1 - \frac{DSM - DTM}{T}\right)}{N}, \qquad S_p = \frac{N_r + N_s}{N} \tag{1}$$

where T is used to compensate the errors in DSM and DTM data.
The road is then found by searching the graph using the best-first method. The method maximizes the length while minimizing the total curvature in a merit function. The function is defined as a weighted summation of parallel measurement for PRSP, image information measurement for PRSP and gap, width similarity measurement between PRSPs, and geometrical linking measurement between PRSPs.
For main roads, on which the system knows that road marks are present based on their classes, the system also extracts roads using detected road marks and zebra crossings. The road marks are linked using a similar method as described in the previous paragraph. This procedure increases the effectiveness and reliability of our system. In complex areas, such as in city centers, the road sides are generally occluded very much, and sometimes it is impossible to identify them. However, the road centerlines are successfully extracted by the system using road marks. In rural and suburban areas, the extracted road using road marks is used by the system to verify the extraction results using 3D parallel edges.
The final step of road extraction is the generation of road network. We inherited the road network topology from VEC25, thus we know how many and which roads come to a road junction, and our system extracts the roads from one junction to another. Once the roads around a junction are extracted, the junction is then reconstructed by the extension and intersection of the roads.

5 Results

The described system is implemented as a standalone software package with a graphic user interface running on SGI platforms. The system reads color stereo imagery, the old road database and other input data, and outputs the extracted roads in 3D Shapefile format that is easily imported by existing GIS software. We have tested the system on a number of images. In this Section, some experimental results of road extraction will be given.
Fig. 8 presents the 3D extraction of road segments in two test sites. Each site covers a portion of a stereo imagery (only the left image is shown). The landscape of Fig. 8a includes open rural, forest and urban areas, while Fig. 8b is mainly a rural scene. Almost all

classes of roads in Switzerland can be found in the two test sites. In Fig. 8a there are about 750 roads (totally around 70 Km) in the overlap area of the stereo images. The system takes about 8h to complete the extraction process. In both test sites, all the roads and junctions in rural areas are correctly and realiably extracted, while in urban areas some roads are not completely extracted due to the highly complexity of the scenes, thus requiring manual interactions. The details of automatic 3D road extraction and junction generation are presented in Fig. 9, where the outdated roads from VEC25 are shown in white, and the extracted roads in black. Fig. 9a, b are examples of road extraction and junction generation in rural areas. In Fig. 9c we show the extracted road in a suburban area. Fig. 9d shows a highway with 4 lanes. The system extracted the lane border lines and lane centerlines through road mark extraction, thus obtaining not only the geometry of the high way, but also its attributes. More examples of 3D road extraction can be found in ZHANG et. al (2001a) and ZHANG et al. (2001b).

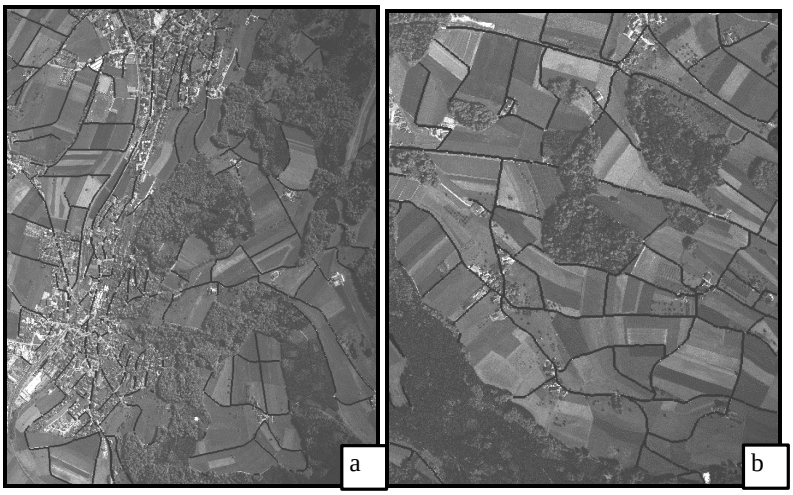

Fig. 8: Test sites and extracted 3D roads and road network. The extracted roads are shown in black.

In order to evaluate the extraction results, a method is developed to compare the extracted roads with reference data. The reference data was measured by the L+T at an analytical plotter. The method matches the vertices of extracted roads to the reference data, and computes coordinate differences. The comparison results for 720 vertices are listed in Table 1. We also match the vertices of the reference data to the extracted roads, however the results are similar to those in Table 1.

Tab. 1: Statistics of absolute difference (in m) between extracted roads and reference data

Statistics	Max	Mean	RMS
DX	1.42	0.32	0.37
DY	1.14	0.20	0.21
DZ	2.37	0.36	0.51

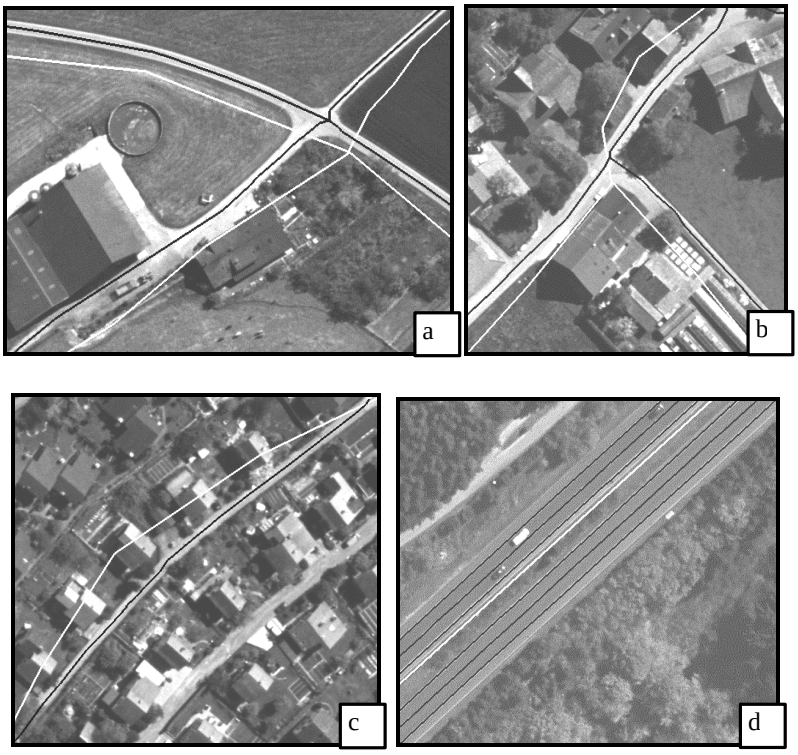

Fig. 9: a) and b) road extraction and junction generation in rural areas, c) road extraction in suburban area, d) extracted lane border lines and lane centerlines of highway through road mark extraction. Extracted roads, lane border lines and lane centerlines are shown in black, the outdated roads from VEC25 in white.

6 Discussion and Conclusion

In this paper, we have presented a knowledge-based image analysis system for road extraction from stereo aerial color images. The system has several advantages over other approaches. It uses existing knowledge, image context, rules and models to restrict the search space, treats each road subclass differently, checks the plausibility of multiple possible hypotheses, therefore provides reliable results. The system contains a set of image processing tools to extract various cues about road existence, and fuses multiple cues and existing information sources. This fusion provides not only complementary information, but also redundant one to account for errors and incomplete results. Working on stereo images, the system makes an early transition from 2D image space to 3D object space. The road hypothesis is generated directly in 3D object space. This not only enables us to apply more geometric criteria to create hypotheses, but also largely reduces the search space, and speeds up the process. The hypotheses are evaluated in images using accumulated knowledge information. Whenever 3D features are incomplete or entirely missing, 2D information from stereo images is used to infer the missing features. By incorporating multiple knowledge, the problematic areas caused by shadows, occlusions etc. can be often handled. Based on the extracted roads the road junctions are generated, thus the system provides an up-to-date road network for practical uses. We also present in this paper the results of road extraction in different landscapes and quantitative analysis using accurate reference data. The comparison of the reconstructed roads with such data showed that the results fulfill the specified accuracy requirements. We are currently working on the derivation of reliability criteria for the extraction results. Our future work will concentrate on road extraction in cities and city centers.

7 Acknowledgement

We acknowledge the financial support for this work and for the project ATOMI by the Swiss Federal Office of Topography, Bern.

8 References

Airault, S., O. Jamet & F. Leymarie (1996): *From Manual to Automatic Stereoplotting: Evaluation of Different Road Network Capture Processes*. International Archives of Photogrammetry and Remote Sensing, Vol. 31, Part B3, pp. 14-18.

Baltsavias, E.P. (1991): *Multiphoto Geometrically Constrained Matching*. Ph.D Thesis, Institute of Geodesy and Photogrammetry, ETH Zurich, Report No. 49.

Baumgartner, A. & H. Hinz (2000): *Multi-Scale Road Extraction Using Local and Global Grouping Criteria*. International Archives of Photogrammetry and Remote Sensing, Vol. 33, Part B3/1, pp. 58-65.

Busch, A. (1994): *Fast Recognition of Lines in Digital Images without User-Supplied Parameters*. International Archives of Photogrammetry and Remote Sensing, Vol. 30, Part 3/1, pp. 91-97.

Eidenbenz, Ch., Ch. Kaeser & E. Baltsavias (2000): *ATOMI – Automated Reconstruction of Topographic Objects from Aerial Images using Vectorized Map Information*. International Archives of Photogrammetry and Remote Sensing, Vol. 33, Part B3/1, pp. 462-471.

Foerstner, W. & L. Pluemer (eds.) (1997): *Semantic Modeling for the Acquisition of Topographic Information from Images and Maps*. Birkhaeuser Verlag, Basel.

Gruen, A., O. Kuebler & P. Agouris (eds.) (1995): *Automatic Extraction of Man-Made Objects from Aerial and Space Images*. Birkhaeuser Verlag, Basel.

Gruen, A., E. P. Baltsavias & O. Henricsson (eds.) (1997): *Automatic Extraction of Man-Made Objects from Aerial and Space Images (II)*. Birkhaeuser Verlag, Basel.

Gruen, A. & H. Li (1997): *Semi-Automatic Linear Feature Extraction by Dynamic Programming and LSB-Snakes.* Photogrammetric Engineering and Remote Sensing, 63(8): 985-995.

Haralick, R.M., L. T. Watson & T. J. Laffey (1983): *The Topographic Primal Sketch*. Int. J. Robotics Research, 2(1): 50-72.

Henricsson, O (1996): *Analysis of Image Structure using Color Attributes and Similarity Relations.* Ph.D Thesis, Institute of Geodesy and Photogrammetry, ETH Zurich, Report No. 59.

Jain, A.K. & R. C. Dubes (eds.) (1988): *Algorithms for Clustering Data*. Prentice-Hall, Inc., New Jersey.

McKeown, D.M. & J. L. Denlinger (1988): *Cooperative Methods for Road Tracking in Aerial Imagery*. Proc. IEEE Computer Vision and Pattern Recognition, pp. 662-672.

Ruskone, R (1996): *Road Network Automatic Extraction by Local Context Interpretation: Application To the Production of Cartographic Data*. Ph.D Thesis, Marne-La-Vallee University.

Vosselman, G. & de M. Gunst (1997): *Updating Road Maps by Contextual Reasoning*. In: A. Gruen, E.P. Baltsavias & O. Henricsson (eds.), Automatic Extraction of Man-Made Objects from Aerial and Space Images (II): 267-276. Birkhäuser Verlag, Basel.

Wang, Y. & J. Trinder (2000): *Road Network Extraction by Hierarchical Grouping*. International Archives of Photogrammetry and Remote Sensing, Vol. 33, Part B3/2, pp. 943-949.

Zhang, C. & E. Baltsavias (2000): *Knowledge-based Image Analysis for 3D Edge Extraction and Road Reconstruction*. International Archives of Photogrammetry and Remote Sensing, Vol. 33, Part B3/2, pp. 1008-1015.

Zhang, C., E. Baltsavias & A. Gruen (2001a): *Knowledge-based Image Analysis for 3D Road Reconstruction*. Asian Journal of Geoinformatic, 1(4):1-14.

Zhang, C., E. Baltsavias & A. Gruen (2001b): *Updating of Cartographic Road Database by Image Analysis.* In: E.P. Baltsavias, A. Gruen & L. V. Gool (eds.), Automatic Extraction of Man-Made Objects from Aerial and Space Images (III), A.A. Balkema Publishers, Lisse (in press).